

Variational study of mass generation and deconfinement in Yang-Mills theory

Giorgio Comitini and Fabio Siringo

*Dipartimento di Fisica e Astronomia dell'Università di Catania,
INFN Sezione di Catania, Via S.Sofia 64, I-95123 Catania, Italy*

(Dated: January 27, 2023)

A very simple variational approach to pure $SU(N)$ Yang-Mills theory is proposed, based on the Gaussian effective potential in a linear covariant gauge. The method provides an analytical variational argument for mass generation. The Landau gauge is found to be optimal for the method which can be improved order by order by a perturbative massive expansion around the optimal trial vacuum. At finite temperature, a weak first-order transition is found (at $T_c \approx 250$ MeV for $N = 3$) where the mass scale drops discontinuously. Above the transition the optimal mass increases linearly as expected for deconfined bosons. The equation of state is found in qualitative agreement with the lattice data, with a latent heat $\Delta H_0 \approx 1.7 T_c$ for $N = 3$.

PACS numbers: 12.38.Aw, 12.38.Lg, 12.38.Bx, 14.70.Dj

I. INTRODUCTION

In the last decades the dynamics of QCD has been under intensive theoretical study, aimed at understanding the properties of matter under the extreme conditions reached by heavy-ion collisions. Our understanding of the phase diagram has further motivated the study of pure $SU(N)$ Yang-Mills theory in the IR and at finite temperature, neglecting quarks as a first approximation. However, despite the important progresses made, we still miss an analytical description of $SU(N)$ theory from first principles, because of the breaking down of standard perturbation theory below the QCD scale.

The numerical simulation of the theory on a lattice has provided many important insights into the gluon dynamics. Among them, the dynamical generation of a gluon mass in the dressed propagator in the Landau gauge[1–8] and the occurrence of a phase transition with the gluons that become deconfined above the critical temperature[9–11]. However, since the numerical simulations can only provide data in the Euclidean space, no direct information can be gained in the Minkowski space where the dynamical properties of the gluon are defined. For instance, no direct proof of confinement can be obtained on the lattice and even the definition of mass can only be regarded as an energy scale without any clear dynamical meaning.

Continuous methods have been developed such as functional renormalization group[12–15], truncation of Dyson-Schwinger equations [16–23] and Hamiltonian approaches[24]. They usually require the numerical solution of integral equations and there is no simple way to extract analytical results from the data.

On the other hand, effective models have been studied analytically, but they are not from first principles and are usually based on some modified quantization procedure[25–28] or different Lagrangians. For instance, adding a gluon mass to the Lagrangian is enough for extending the validity of perturbation theory down to the deep IR, yielding a very good overall picture of Yang-Mills theory at one loop[29–31]. In the context of back-

ground field methods the added gluon mass has provided a good description of the phase diagram at finite temperature, enforcing the idea that most of the non-perturbative effects can be embedded in the gluon-mass parameter[32–35]. While those models are important for understanding the physics of gluons, their comparison with the lattice data is not clear since the original Lagrangians are different. Thus, there is a growing interest in the study of analytical approaches to the exact $SU(N)$ theory.

In this paper, we discuss a very simple variational approach to $SU(N)$ theory, based on the Gaussian effective potential (GEP) in a linear covariant gauge. We do not modify the original Lagrangian of the theory but optimize the perturbative expansion by a variational argument, yielding a calculational analytical method that already provides very important predictions at the lowest orders of the approximation. Among the main results achieved by the present study we mention: i) a variational argument for mass generation; ii) the prediction of a first-order deconfinement transition at $T_c \approx 250$ MeV for $N = 3$; iii) the formal definition of a perturbative expansion around the optimized vacuum, allowing for an order-by-order improvement of the approximation.

The original approach of Ref.[36] is here improved and extended to finite temperature, yielding analytical results up to a one-dimensional numerical integration that is required for the thermal functions. The perturbative expansion around the vacuum turns out to be the massive expansion developed in Refs.[37–40] which was found in excellent agreement with the lattice data[41]. Thus, the present study enforces the validity of that expansion and provides a variational argument for its derivation. Moreover, while by itself the massive expansion did not give a genuine proof of mass generation, the variational nature of the GEP can be used as a tool for demonstrating that the standard vacuum of Yang-Mills theory is unstable towards the vacuum of massive gluons[36]. Moreover, the Landau gauge is shown to be the optimal gauge for the method, as already found for the scalar QED[42]

The expansion has been extended to finite temperature

in Ref.[40] allowing for a direct calculation of the gluon damping rate in the IR and providing a direct proof of confinement. While in that study the zeroth order mass parameter was kept fixed, at finite temperature the GEP provides a free energy and allows us to determine the trial mass parameter variationally, as a function of temperature. The optimal mass scale is found discontinuous at the deconfinement transition, leading to an enhancement of the mass decrease that was already found in Ref.[40], in agreement with the observed behavior of the Debye mass in lattice simulations[10].

The GEP is the energy density of a trial Gaussian vacuum functional that is centered at a given average value of the field. The width of the functional is given by the mass of the trial free theory and is determined variationally at each value of the average field, yielding an effective potential that has been studied by several authors, mainly in the context of spontaneous symmetry breaking and scalar theories[42–58]. While the GEP is a genuine variational method[45, 46], several extensions to higher orders have been proposed[55–58]. The idea of an expansion around the optimized vacuum of the GEP is not new[59] but has not been developed further. Expanding around the optimized massive vacuum of the GEP, the unconventional massive expansion of Refs.[37–39] is recovered in a natural way[36]. Thus, the phenomenological success of the expansion might be due to the variational choice of a zeroth order vacuum which incorporates most of the non-perturbative effects, leaving a residual interaction term that can be treated by perturbation theory.

One of the important merits of the GEP is its paradox of being a pure variational method disguised as a perturbative calculation, making use of the standard graphs of perturbation theory. Moreover, in the present context, the calculation is highly simplified by the assumption that the average of the gauge field is zero at the minimum of the potential. In other words, we only need the effective potential at its minimum where it is a function $V(m)$ of the trial mass parameter m .

The paper is organized as follows: in Sec.II the general formalism and the renormalization scheme are discussed in the simple case of a scalar theory where standard well known results are recovered by the method; in Sec.III the GEP for pure $SU(N)$ Yang-Mills theory is studied at $T = 0$, providing a simple variational argument for mass generation; in Sec.IV the GEP is extended to finite temperature and the phase transition is discussed; a general discussion and a summary of the results follow in Sec.V.

II. GEP AND MASS GENERATION IN THE SCALAR THEORY

In order to illustrate the method and the renormalization scheme, in this section we revise the formalism for the simple case of a self-interacting scalar theory[45] where the effective potential is well known and is given

by three vacuum graphs as shown in Fig. 1. Most of the arguments developed here are quite general and will be used in the next sections.

Let us consider the Lagrangian

$$\mathcal{L} = \frac{1}{2}\phi(-\partial^2 - m_B^2)\phi - \frac{\lambda}{4!}\phi^4 \quad (1)$$

where m_B is a bare mass. We can split the total Lagrangian as $\mathcal{L} = \mathcal{L}_0 + \mathcal{L}_{int}$ where the trial quadratic part is

$$\mathcal{L}_0 = \frac{1}{2}\phi(-\partial^2 - m^2)\phi \quad (2)$$

and describes a free scalar particle with a trial mass $m \neq m_B$. The new interaction follows as

$$\mathcal{L}_{int} = -\frac{\lambda}{4!}\phi^4 - \frac{1}{2}(m_B^2 - m^2)\phi^2 \quad (3)$$

so that the total Lagrangian is left unchanged. If we neglect the interaction, then a free Hamiltonian \mathcal{H}_0 is derived from \mathcal{L}_0 and its ground state $|m\rangle$ satisfies

$$\mathcal{H}_0 |m\rangle = E_0(m) |m\rangle \quad (4)$$

and depends on the trial mass m . Restoring the interaction \mathcal{L}_{int} , the full Hamiltonian reads $\mathcal{H} = \mathcal{H}_0 + \mathcal{H}_{int}$ and by standard perturbation theory, the first-order energy of the ground state reads

$$E_1(m) = E_0(m) + \langle m | \mathcal{H}_{int} | m \rangle = \langle m | \mathcal{H} | m \rangle \quad (5)$$

and is equivalent to the first-order effective potential $V_1(m)$ evaluated by perturbation theory in the covariant formalism with the interaction \mathcal{L}_{int} . Thus, the stationary condition

$$\frac{\partial V_1(m)}{\partial m} = \frac{\partial E_1(m)}{\partial m} = 0 \quad (6)$$

gives the best value of m that minimizes the vacuum energy of the ground state $|m\rangle$.

While being a pure variational method, the first-order effective potential $V_1(m) = E_1(m)$ can be evaluated by the sum of all the vacuum graphs up to first order (the three loop graphs in Fig. 1). The resulting optimized effective potential is the GEP. Usually, the effective potential is evaluated for any value of the average $\varphi = \langle \phi \rangle$ and the best m also depends on that average. If the

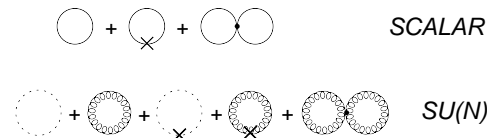


Figure 1: Vacuum graphs contributing to the GEP for the scalar theory (first row) and pure $SU(N)$ Yang-Mills theory (second row).

symmetry is not broken, then the minimum of the effective potential is at $\varphi = 0$ where $V_1(m)$ is a function of the trial mass, to be fixed by the stationary condition Eq.(6). We assume that the gauge symmetry is not broken in Yang-Mills theory so that $V_1(m)$ at $\varphi = 0$ is the effective potential we are interested in.

The variational nature of the method ensures that the true vacuum energy is smaller than the minimum of $V_1(m)$. At the minimum, $|m\rangle$ provides an approximation for the vacuum and is given by the vacuum of a free massive scalar particle with mass equal to the optimized mass parameter $m \neq m_B$. Of course, the optimal state $|m\rangle$ is just a first approximation and the actual vacuum is much richer. However, we expect that a perturbative expansion around that approximate vacuum would be the best choice for the Lagrangian \mathcal{L} , prompting towards an expansion with an interaction \mathcal{L}_{int} and a free part \mathcal{L}_0 that depend on m and can be optimized by a clever choice of the parameter m . Different strategies have been proposed for the optimization, ranging from the stationary condition of the GEP, Eq.(6), to Stevenson's principle of minimal sensitivity[60]. A method based on the minimal variance has been recently proposed for QCD and other gauge theories[56, 61–65]. In all those approaches, the underlying idea is that an optimal choice of m could minimize the effect of higher orders in the expansion. Since the total Lagrangian does not depend on m , the physical observables are expected to be stationary at the optimal m , thus suggesting the use of stationary conditions for determining the free parameter. As a matter of fact, if all graphs were summed up exactly, then the dependence on m would cancel in the final result, so that the strength of that dependence measures the weight of the neglected graphs at any order.

Leaving aside the problem of the best choice of m , we observe that at $\varphi = 0$ the calculation of the first-order effective potential $V_1(m)$ is quite straightforward and follows from the first-order expansion of the effective action $\Gamma(\varphi)$

$$e^{i\Gamma(\varphi)} = \int_{1PI} \mathcal{D}_\phi e^{iS_0(\phi+\varphi)+iS_{int}(\phi+\varphi)} \quad (7)$$

where the functional integral is the sum of all one-particle irreducible (1PI) graphs and $S = S_0 + S_{int}$ is the action. The effective potential then follows as $V(m) = -\Gamma(0)/\mathcal{V}_4$ where \mathcal{V}_4 is a total space-time volume. The sum of graphs up to first order gives the first-order effective potential $V_1(m)$ which is the GEP when optimized by Eq.(6).

At finite temperature, the effective potential is replaced by a density of free energy $\mathcal{F}(T, m)$ according to

$$e^{-\beta[\mathcal{V}_3 \mathcal{F}(T, m)]} = \int \mathcal{D}_\phi e^{(S_0+S_{int})} \quad (8)$$

where the action $S = S_0 + S_{int}$ is the integral over imaginary time τ

$$S = \int_0^\beta d\tau \int d^3x \mathcal{L}, \quad (9)$$

$\beta = 1/T$ and \mathcal{V}_3 is a total three-dimensional space volume. The perturbative expansion of the free energy follows by the same connected graphs contributing to the effective potential, with loop integrals replaced by a sum over discrete frequencies and a three-dimensional integration. In the limit $T \rightarrow 0$ the effective potential is recovered as $V(m) = \mathcal{F}(0, m)$ and each thermal graph gives the corresponding vacuum term. Because of the one to one correspondence of the graphs we can easily switch from the thermal to the vacuum formalism when required. Moreover, at finite temperature, the GEP maintains its genuine variational nature. In the Hamiltonian formalism, the variational argument that follows Eq.(5) can be generalized by Bogolubov's inequality

$$\mathcal{F} \leq \mathcal{F}_0 + \frac{1}{\mathcal{V}_3} \frac{\text{Tr} [\mathcal{H}_{int} \exp(-\beta\mathcal{H}_0)]}{\text{Tr} [\exp(-\beta\mathcal{H}_0)]} = \mathcal{F}_1 \quad (10)$$

while in the Lagrangian formalism the same result is found by Jensen-Feynman inequality

$$\mathcal{F} \leq \mathcal{F}_0 - \frac{1}{\beta\mathcal{V}_3} \frac{\int \mathcal{D}_\phi S_{int} e_0^S}{\int \mathcal{D}_\phi e_0^S} = \mathcal{F}_1 \quad (11)$$

where \mathcal{F}_0 is the free energy obtained by the trial Lagrangian \mathcal{L}_0 while \mathcal{F}_1 is the first order approximation which becomes the GEP when optimized. The two inequalities tell us that the expansion must be truncated at first order for a genuine variational approximation. Here and in the next section, when not specified, we will deal with the effective potential and with the renormalization of the vacuum graphs at zero temperature. The thermal corrections are finite and do not require any further renormalization.

Since we are interested in the massless Yang-Mills theory, we set $m_B = 0$ in the interaction Eq.(3) and study a massless scalar theory as a toy model for the problem of mass generation. The vertices of the theory can be read from \mathcal{L}_{int} in Eq.(3) where we set $m_B = 0$ and are used in Fig.1 in the vacuum graphs. The usual four-point vertex $-\lambda$ is accompanied by the counterterm $\delta\Gamma = m^2$ that is denoted by a cross in the graphs. This counterterm must be regarded as part of the interaction so that the expansion is not loopwise and we find one-loop and two-loop graphs summed together in the first-order effective potential. That is where the non-perturbative nature of the method emerges since the expansion is not in powers of λ but of the whole interaction \mathcal{L}_{int} . The zeroth order (massive) propagator Δ_m follows from \mathcal{L}_0

$$\Delta_m(p) = \frac{1}{p^2 - m^2} \quad (12)$$

and is shown as a straight line in the vacuum graphs.

The tree term is the classical potential and vanishes in the limit $\varphi \rightarrow 0$. The first one-loop graph in Fig.1 gives the standard one-loop effective potential, containing some effects of quantum fluctuations. It must be added to the second one-loop graph in Fig.1, the crossed graph containing one insertion of the counterterm.

It is instructive to see that the exact sum of all one-loop graphs with n insertions of the counterterm gives the standard vacuum energy of a massless particle. In other words, if we sum all the crossed one-loop graphs the dependence on m disappears and we are left with the standard one-loop effective potential of Weinberg and Coleman[66] $V_{1L}^0 = -\Gamma_{1L}^0/\mathcal{V}_4$ where Γ_{1L}^0 is the standard one-loop effective action at $\varphi = 0$

$$e^{i\Gamma_{1L}^0} = \int \mathcal{D}\phi e^{i \int \frac{1}{2} \phi (-\partial^2) \phi d^4x} \sim [\text{Det}(\Delta_0^{-1})]^{-\frac{1}{2}} \quad (13)$$

and $\Delta_0^{-1} = p^2$ is the free-particle propagator of a massless scalar particle. Up to an additive constant, not depending on m , Eq.(13) can be written as

$$V_{1L}^0 = \frac{-i}{2\mathcal{V}_4} \text{Tr} \log(\Delta_m^{-1} + m^2) \quad (14)$$

then expanding the log we obtain a *massive expansion*

$$V_{1L}^0 = \frac{-i}{2\mathcal{V}_4} \text{Tr} \left\{ \log(\Delta_m^{-1}) - \sum_{n=1}^{\infty} \frac{(-m^2 \Delta_m)^n}{n} \right\} \quad (15)$$

that is shown pictorially in Fig.2 as a sum of crossed one-loop vacuum graphs. While the sum cannot depend on m , if we truncate the expansion at any finite order we obtain a function of the mass parameter. As a test of consistency, one can easily check that, once renormalized as described below, the sum of all the crossed one-loop vacuum graphs in Fig.2 gives zero exactly.

The calculation of the GEP requires the sum of only the first two terms of Eq.(15), the two one-loop graphs in Fig.1. We cannot add higher-order terms without spoiling the variational method since the average value of the Hamiltonian in the trial state $|m\rangle$ is $E_1(m) = V_1(m)$, according to Eq.(5). Using the identity

$$\Delta_m = -\frac{\partial}{\partial m^2} \log(\Delta_m^{-1}) \quad (16)$$

the sum of one-loop graphs in Fig.1 can be written as

$$V_{1L}(m) = \left(1 - m^2 \frac{\partial}{\partial m^2}\right) K(m) = K(m) - \frac{1}{2} m^2 J(m) \quad (17)$$

where $K(m)$ and $J(m)$ are defined as

$$\begin{aligned} K(m) &= \frac{-i}{2\mathcal{V}_4} \text{Tr} \log(\Delta_m^{-1}) \\ J(m) &= \frac{i}{\mathcal{V}_4} \text{Tr} \Delta_m \end{aligned} \quad (18)$$

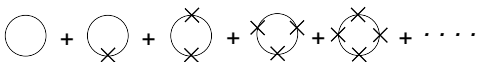


Figure 2: Pictorial display of the right hand side of Eq.(15).

and because of Eq.(16), satisfy the identity

$$\frac{\partial K(m)}{\partial m^2} = \frac{1}{2} J(m). \quad (19)$$

At $T = 0$ they can be written as explicit diverging integrals

$$\begin{aligned} K(m) &= \frac{1}{2i} \int \frac{d^4p}{(2\pi)^4} \log(-p^2 + m^2) \\ J(m) &= -i \int \frac{d^4p}{(2\pi)^4} \frac{1}{-p^2 + m^2} \end{aligned} \quad (20)$$

to be regularized in some renormalization scheme. At finite temperature Eq.(19) still holds, but the integrals acquire a finite additive thermal part.

We recognize $K(m)$ as the standard one-loop effective potential of Weinberg and Coleman for a massive scalar particle in the limit $\varphi \rightarrow 0$. This term contains the quantum fluctuations at one-loop. The second term in Eq.(17) is a correction coming from the counterterm and arises because the exact Lagrangian was massless.

The calculation of the GEP also requires the two-loop graph in Fig.1 that is first-order in λ . It can be recovered from the crossed one-loop graph by just substituting the vertex $-m^2$ with the seagull one-loop self energy Σ_{1L} that reads[56]

$$\Sigma_{1L} = \frac{\lambda}{2} J(m) \quad (21)$$

and adding a 1/2 symmetry factor. The resulting two-loop term is

$$V_{2L}(m) = \frac{\lambda}{8} [J(m)]^2. \quad (22)$$

The GEP follows as the sum $V_{1L} + V_{2L}$

$$V_G(m) = K(m) - \frac{1}{2} m^2 J(m) + \frac{\lambda}{8} [J(m)]^2. \quad (23)$$

At this stage we have just recovered the GEP in the limit $\varphi \rightarrow 0$ and Eq.(23) agrees with the well known GEP in that limit[45, 55, 56, 58].

More precisely, V_G is the GEP when m is optimized by the stationary condition Eq.(6) that reads

$$\frac{\partial V_G(m)}{\partial m^2} = \frac{1}{2} \left(\frac{\partial J(m)}{\partial m^2} \right) \left[\frac{\lambda J(m)}{2} - m^2 \right] = 0 \quad (24)$$

yielding the usual gap equation of the GEP

$$m^2 = \frac{\lambda J(m)}{2}. \quad (25)$$

From a mere formal point of view, the GEP predicts the existence of a mass for the massless scalar theory. That is of special interest because for $m_B = 0$ the Lagrangian in Eq.(1) has no energy scale, just like Yang-Mills theory and QCD in the chiral limit. Thus, it can be regarded

as a toy model for the more general problem of mass generation and chiral symmetry breaking.

Actually, the integrals J , K are badly diverging, and a mass scale arises from the regulator that must be inserted in order to get a meaningful theory. By dimensional regularization, setting $d = 4 - \epsilon$, the integral J is

$$J(m) = -\frac{m^2}{16\pi^2} \left[\frac{2}{\epsilon} + \log \frac{\bar{\mu}^2}{m^2} + 1 + \mathcal{O}(\epsilon) \right] \quad (26)$$

where $\bar{\mu} = (2\sqrt{\pi}\mu)\exp(-\gamma/2)$ is an arbitrary scale. Integrating Eq.(19) and neglecting an integration constant (that does not depend on m)

$$K(m) = -\frac{m^4}{64\pi^2} \left[\frac{2}{\epsilon} + \log \frac{\bar{\mu}^2}{m^2} + \frac{3}{2} + \mathcal{O}(\epsilon) \right]. \quad (27)$$

If we follow the usual approach of Weinberg and Coleman[66], the divergences must be absorbed by the physical renormalized parameters. Thus, let us define a *physical* renormalized energy scale Λ as

$$\log \Lambda^2 = \log \bar{\mu}^2 + \frac{2}{\epsilon} + 1 \quad (28)$$

and write the integrals K , J as simply as

$$\begin{aligned} J(m) &= \frac{m^2}{16\pi^2} \log \frac{m^2}{\Lambda^2} \\ K(m) &= \frac{m^4}{64\pi^2} \left[\log \frac{m^2}{\Lambda^2} - \frac{1}{2} \right]. \end{aligned} \quad (29)$$

This approach is the same that is usually followed in lattice simulations of QCD: the lattice provides a scale that can be changed without affecting the physical scale which remains fixed at a phenomenological value. Here we assume that Λ is some unknown energy scale that must be given by the phenomenology.

We observe that by our renormalization scheme the standard one-loop effective potential is recovered, since that is equal to $K(m)$ in Eq.(29) and can be recognized as

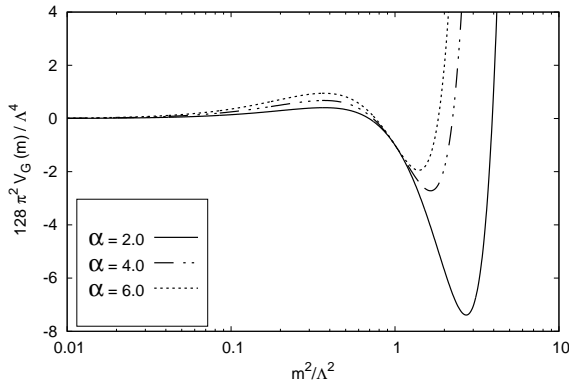


Figure 3: The GEP of Eq.(30) is shown for different values of the effective coupling α .

the mass-dependent term of the standard one-loop effective potential in the limit $\varphi \rightarrow 0$. That term has a relative maximum at $m = 0$, is negative for $m < \Lambda \exp(1/4)$ and has the absolute minimum at $m = \Lambda$. Thus, the one-loop effective potential would predict a massive vacuum if the symmetry were not broken and the physical vacuum were at $\varphi = 0$ (which is not the case in the standard model since the symmetry of the Higgs field is broken).

The full renormalized GEP is finite in terms of the physical scale Λ and can be written as

$$V_G(m) = \frac{m^4}{128\pi^2} \left[\alpha \left(\log \frac{m^2}{\Lambda^2} \right)^2 - 2 \log \frac{m^2}{\Lambda^2} - 1 \right] \quad (30)$$

where α is the effective coupling $\alpha = \lambda/(16\pi^2)$.

The behavior of the potential is shown in Fig.3. For any coupling α , the point $m = 0$ is a relative minimum while the potential has a relative maximum at $m^2/\Lambda^2 = 1/e$. The absolute minimum is at $m^2 = m_0^2 = \Lambda^2 \exp(2/\alpha)$ where $128\pi^2 V_G(m_0) = -m_0^4 < 0$. The two stationary points $m = \Lambda/\sqrt{e}$ and $m = m_0$ are the points where the first or second factor in Eq.(24) is zero, respectively. Thus the absolute minimum m_0 is the solution of the gap equation, Eq.(25). However, since the original theory has no scale, the quantitative value of m remains arbitrary as it depends on the unknown scale Λ . We can only predict that, since the GEP provides a genuine variational approximation for the vacuum energy, the massless vacuum must be unstable towards the vacuum of a massive scalar particle.

A nice feature of the GEP is that its value at the minima does not depend on the coupling, up to an overall factor. That is made evident when we express the renormalized GEP in terms of the optimal physical mass m_0 , eliminating the unknown scale Λ in Eq.(30)

$$V_G(m) = \frac{m^4}{128\pi^2} \left[\alpha \left(\log \frac{m^2}{m_0^2} \right)^2 + 2 \log \frac{m^2}{m_0^2} - 1 \right]. \quad (31)$$

We observe that the stationary point m_0 is the physical mass that emerges as the pole of the self-consistent propagator. Actually, up to first order, the self-energy is the sum of the tree-level counterterm $-m^2$ and the seagull graph Σ_{1L} in Eq.(21), so that the self-consistency condition $m = m_0$ is equivalent to the vanishing of the first-order self energy[56]

$$\Sigma_1 = -m^2 + \frac{\lambda}{2} J(m) = 0 \quad (32)$$

which is just the stationary condition Eq.(25) satisfied by m_0 . Lattice data confirm the existence of a finite mass in the limit $m_B^2 \rightarrow 0^+$ of the unbroken-symmetry theory. An unstable minimum is always present at $m = 0$ and it becomes the only minimum left in the limit $\Lambda \rightarrow \infty$ when the triviality of the scalar theory is recovered.

III. GEP AND MASS GENERATION IN SU(N) THEORY

The Lagrangian of pure SU(N) Yang-Mills theory can be written as

$$\mathcal{L} = \mathcal{L}_{YM} + \mathcal{L}_{fix} + \mathcal{L}_{FP} \quad (33)$$

where \mathcal{L}_{YM} is the Yang-Mills term

$$\mathcal{L}_{YM} = -\frac{1}{2} \text{Tr} \left(\hat{F}_{\mu\nu} \hat{F}^{\mu\nu} \right) \quad (34)$$

\mathcal{L}_{fix} is a gauge fixing term and \mathcal{L}_{FP} is the ghost Lagrangian arising from the Faddeev-Popov determinant. In terms of the gauge fields, the tensor operator $\hat{F}_{\mu\nu}$ is

$$\hat{F}_{\mu\nu} = \partial_\mu \hat{A}_\nu - \partial_\nu \hat{A}_\mu - ig [\hat{A}_\mu, \hat{A}_\nu] \quad (35)$$

where

$$\hat{A}^\mu = \sum_a \hat{T}_a A_a^\mu \quad (36)$$

and the generators of SU(N) satisfy the algebra

$$[\hat{T}_a, \hat{T}_b] = if_{abc} \hat{T}_c \quad (37)$$

with the structure constants normalized according to

$$f_{abc} f_{dbc} = N \delta_{ad}. \quad (38)$$

If a generic linear covariant gauge-fixing term is chosen

$$\mathcal{L}_{fix} = -\frac{1}{\xi} \text{Tr} \left[(\partial_\mu \hat{A}^\mu)(\partial_\nu \hat{A}^\nu) \right], \quad (39)$$

where $\xi > 0$ is an arbitrary positive number, the total action can be written as $\mathcal{S}_{tot} = \mathcal{S}_0 + \mathcal{S}_I$ where the free-particle term is

$$\begin{aligned} \mathcal{S}_0 = & \frac{1}{2} \int A_{a\mu}(x) \delta_{ab} \Delta_0^{-1 \mu\nu}(x, y) A_{b\nu}(y) d^d x d^d y \\ & + \int \omega_a^*(x) \delta_{ab} \mathcal{G}_0^{-1}(x, y) \omega_b(y) d^d x d^d y \end{aligned} \quad (40)$$

and the interaction is

$$\mathcal{S}_I = \int d^d x [\mathcal{L}_{3g} + \mathcal{L}_{4g} + \mathcal{L}_{gh}] \quad (41)$$

with the usual local interaction terms that read

$$\begin{aligned} \mathcal{L}_{3g} &= -g f_{abc} (\partial_\mu A_{a\nu}) A_b^\mu A_c^\nu \\ \mathcal{L}_{4g} &= -\frac{1}{4} g^2 f_{abc} f_{ade} A_{b\mu} A_{c\nu} A_d^\mu A_e^\nu \\ \mathcal{L}_{gh} &= -g f_{abc} (\partial_\mu \omega_a^*) \omega_b A_c^\mu. \end{aligned} \quad (42)$$

In Eq.(40), Δ_0 and \mathcal{G}_0 are the standard free-particle propagators for gluons and ghosts and their Fourier transforms are

$$\begin{aligned} \Delta_0^{\mu\nu}(p) &= \Delta_0(p) [t^{\mu\nu}(p) + \xi \ell^{\mu\nu}(p)] \\ \Delta_0(p) &= \frac{1}{-p^2}, \quad \mathcal{G}_0(p) = \frac{1}{p^2}. \end{aligned} \quad (43)$$

Here the transverse and longitudinal projectors are defined as

$$t_{\mu\nu}(p) = g_{\mu\nu} - \frac{p_\mu p_\nu}{p^2}; \quad \ell_{\mu\nu}(p) = \frac{p_\mu p_\nu}{p^2} \quad (44)$$

where $g_{\mu\nu}$ is the metric tensor.

As discussed in Refs.[38, 39], an unconventional massive expansion can be introduced by adding and subtracting mass terms $\delta\mathcal{S}_i$ in the total action, just like we did for the scalar theory in Eqs.(2),(3). The method can be generalized by redefining the free and interacting parts of the action

$$\begin{aligned} \mathcal{S}_0 &\rightarrow \mathcal{S}_0 - \sum_i \delta\mathcal{S}_i \\ \mathcal{S}_I &\rightarrow \mathcal{S}_I + \sum_i \delta\mathcal{S}_i. \end{aligned} \quad (45)$$

For the gluon we can take

$$\delta\mathcal{S}_g = \frac{1}{2} \int A_{a\mu}(x) \delta_{ab} \delta\Gamma^{\mu\nu}(x, y) A_{b\nu}(y) d^d x d^d y \quad (46)$$

where the vertex function $\delta\Gamma^{\mu\nu}$ is given by a shift of the inverse propagator

$$\delta\Gamma^{\mu\nu}(x, y) = \left[\Delta_0^{-1 \mu\nu}(x, y) - \Delta_m^{-1 \mu\nu}(x, y) \right] \quad (47)$$

and $\Delta_m^{\mu\nu}$ is the massive free-particle propagator

$$\begin{aligned} \Delta_m^{-1 \mu\nu}(p) &= \Delta_m^T(p)^{-1} t^{\mu\nu}(p) + \Delta_m^L(p)^{-1} \ell^{\mu\nu}(p) \\ \Delta_m^T(p) &= \frac{1}{-p^2 + m^2}, \quad \Delta_m^L(p) = \frac{\xi}{-p^2 + m_L^2} \end{aligned} \quad (48)$$

As a general variational ansatz, the two masses m and m_L can be different. We also have the freedom to insert a mass shift $\delta\mathcal{S}_{gh}$ for the ghost

$$\delta\mathcal{S}_{gh} = \int \omega_a^*(x) \delta_{ab} \delta\Gamma(x, y) \omega_b(y) d^d x d^d y \quad (49)$$

together with its counterterm $\delta\Gamma$

$$\delta\Gamma(x, y) = [\mathcal{G}_0^{-1}(x, y) - \mathcal{G}_M^{-1}(x, y)] \quad (50)$$

where \mathcal{G}_M would be a massive ghost propagator

$$\mathcal{G}_M = \frac{1}{p^2 - M^2}. \quad (51)$$

In the massive expansion of Refs.[38, 39, 41] no ghost and longitudinal masses were inserted (i.e. $M = m_L = 0$). Only the pole of the transverse free-particle propagator was shifted and compensated by inserting a transverse counterterm

$$\delta\Gamma^{\mu\nu}(p) = -m^2 t^{\mu\nu}(p) \quad (52)$$

among the vertices of the interaction. The gauge-dependent longitudinal part of the gluon propagator was

left unchanged and equal to the exact result $\Delta_0^L(p) = \xi/(-p^2)$. As shown in Ref.[41] that massive expansion is in very good agreement with the data of lattice simulations. However, that choice could be just sub-optimal and a more general ansatz could be considered.

While the mass parameters might appear as independent variational parameters, there are strong constraints that arise from the requirement that the trial action S_0 makes sense and is the reasonable zeroth order action of a physical system. While not necessary, that requirement is expected to improve the reliability of the variational method. Moreover, the existence of ghosts in the covariant formalism and the appearance of states with negative norm in the Hamiltonian formalism might limit the use of Jensen-Feynman inequality Eq.(11) and Bogolubov's inequality Eq.(10), respectively, unless we have a very strong physical evidence about the safe cancellation of the unphysical degrees of freedom in the averages. Thus, we must ensure that the ghost cancels the unphysical degrees of freedom in the zeroth order trial physical system described by the free action S_0 . It is not difficult to guess that the cancellation can only happen if we ensure that the propagators have the same masses by imposing the condition $M = m_L = m$. That constraint emerges as almost mandatory at finite temperature. At $T = 0$ we could just set $M = 0$ in the ghost propagators and omit the constant ghost loops. Actually, if the ghost mass parameter M were regarded as an independent variational mass parameter, then its gap equation would give $M = 0$ because there are not ghost-gluon vertices in the first order effective potential. On the other hand, at finite temperature, the ghost loops depend on temperature and cannot be omitted even when $M = 0$. If the ghost must cancel the effects of an unphysical longitudinal gluon and of one transversal degree of freedom they must have the same mass. For instance if $M = 0$ and $T \ll m$ the light ghost would give an enhanced (wrong sign) contribution to the free energy compared to the gluon that would be almost frozen. The free energy would become an increasing function of temperature yielding a negative entropy. Thus, the ghost mass parameter M cannot be regarded as an independent variational parameter but must be set equal to the gluon value $m = m_L$. A finite longitudinal mass might seem odd, because of the gauge invariance of the Yang-Mills Lagrangian, but S_0 is not BRST invariant anyway in presence of a gluon mass term. While the exact effective potential must be gauge invariant, we expect that at any finite order of the massive expansion, the approximated effective potential might depend on the gauge parameter ξ . It is encouraging to see that up to one-loop the result turns out to be gauge invariant, as it should be if S_0 described a real physical system.

The constraint $M = m = m_L$ is satisfied if, according to Eqs.(47),(50), we use the following counterterms

$$\begin{aligned} \delta\Gamma^{\mu\nu}(p) &= -m^2 t^{\mu\nu}(p) - \frac{m^2}{\xi} \ell^{\mu\nu}(p) \\ \delta\Gamma(p) &= m^2 \end{aligned} \quad (53)$$

with free propagators given by Eqs.(48),(51) where we set $M = m$ and $m_L = m$. The calculation of the GEP follows the same steps as for the scalar theory. The GEP is obtained as the first-order effective potential in the covariant formalism, including the counterterms among the interaction vertices and in the limit of a vanishing background field, i.e. assuming that $\langle A_{a\mu} \rangle = 0$ since gauge symmetry is not broken in the vacuum. The effective action reads

$$e^{i\Gamma(a)} = \int_{1PI} \mathcal{D}_{A,\omega} e^{iS_0(a+A,\omega) + iS_{int}(a+A,\omega)} \quad (54)$$

and the effective potential follows as $V = -\Gamma(0)/\mathcal{V}_4$ and is the sum of all connected 1PI vacuum graphs. The first order graphs contributing to the GEP are shown in the second row of Fig. 1.

The zeroth order gluon and ghost loops in Fig. 1 give

$$V_0 = \frac{i}{2\mathcal{V}_4} \log \text{Det} \Delta_m^{\mu\nu} - \frac{i}{\mathcal{V}_4} \log \text{Det} \mathcal{G}_m. \quad (55)$$

The determinant of $\Delta_m^{\mu\nu}$ can be split as the product of determinants in the orthogonal Lorentz subspaces, $\text{Det} \Delta_m^{\mu\nu} = \text{Det}[\Delta_m^T t^{\mu\nu}] \text{Det}[\Delta_m^L \ell^{\mu\nu}]$, yielding

$$V_0 = \frac{i(d-1)}{2\mathcal{V}_4} \text{Tr} \log \Delta_m^T + \frac{i}{2\mathcal{V}_4} \text{Tr} \log \Delta_m^L - \frac{i}{\mathcal{V}_4} \text{Tr} \log \mathcal{G}_m. \quad (56)$$

where $d = 4$ in a four dimensional space-time. Since $\Delta_m^T = \Delta_m^L/\xi = -\mathcal{G}_m$, up to the constant gauge dependent (infinite) term $\text{Tr} \log \xi$, which is canceled by an equal factor in the normalization of the Faddeev-Popov functional, the ghost cancels the longitudinal term and one transverse gluon degree of freedom, yielding

$$V_0(m) = N_A(d-2)K(m). \quad (57)$$

where $N_A = N^2 - 1$. The crossed one-loop graphs in Fig. 1 are obtained by one insertion of the counterterms. The identity Eq.(16) still holds for \mathcal{G}_m , changes its sign for Δ_m^T and contains the extra factor $-1/\xi$ for Δ_m^L . Thus, inserting the counterterms of Eq.(53) in the loops, we observe that acting with the operator $-m^2(\partial/\partial m^2)$ on each single term in Eq.(56) generates the corresponding crossed loop. Then, as in Eq.(17), using Eq.(16), the sum of all one-loop graphs (zeroth and first order) can be written as

$$\begin{aligned} V_{1L}(m) &= \left(1 - m^2 \frac{\partial}{\partial m^2}\right) V_0(m) = \\ &= N_A(d-2) \left[K(m) - \frac{1}{2} m^2 J(m) \right] \end{aligned} \quad (58)$$

which is the same result of the scalar theory Eq.(17) multiplied by the number of physical gluons $N_A(d-2)$. The functions $K(m)$ and $J(m)$ were defined in Eq.(20) and their explicit regularized expression were given in Eq.(29). The formal result of Eq.(58) is also valid at

finite temperature, since Eq.(16) still holds when the integrals K, J acquire a thermal part. Eq.(58) gives a one-loop free energy which is gauge invariant and does not contain unphysical degrees of freedom, desirable features of a trial free action.

The first-order effective potential also includes the two-loop gluon graph in Fig. 1 which is not gauge invariant. Its calculation is formally different in the finite temperature formalism and will be studied in the next section. Here, we examine the vacuum part that contributes to the GEP at $T = 0$ and is relevant for discussing the issue of mass generation. Inserting the seagull one-loop graph[65]

$$\Pi_{1L} = -\frac{(d-1)Ng^2}{d} [\xi + (d-1)] J(m) \quad (59)$$

the two-loop term reads

$$V_{2L}(m) = \frac{N_A Ng^2(d-1)}{4d} (d-1+\xi)^2 [J(m)]^2 \quad (60)$$

and is always positive and minimal in the Landau gauge, for $\xi = 0$.

Setting $d = 4$ and adding up Eq.(58) and Eq.(60), in terms of the new effective coupling α

$$\alpha = \frac{27Ng^2}{64\pi^2} = \frac{27N}{16\pi} \alpha_s, \quad \alpha_s = \frac{g^2}{4\pi} \quad (61)$$

the gauge-dependent GEP can be written as

$$\frac{V_G(m)}{2N_A} = K(m) - \frac{m^2}{2} J(m) + 2\pi^2 \alpha \left[\left(1 + \frac{\xi}{3}\right) J(m) \right]^2 \quad (62)$$

which is the same identical result obtained in Eq.(23) for the scalar theory, provided that the effective coupling $\alpha(1 + \xi/3)^2$ is replaced by $\lambda/(16\pi^2)$.

The gauge dependence was expected, since the present trial zeroth order action does not leave the longitudinal gluon propagator Δ^L unchanged and massless, as would be imposed by gauge invariance. However, the variational nature of the method allows us to look for the best gauge where the ansatz gives a better approximation. We can use ξ as a further variational parameter and assuming that $\xi > 0$, the GEP is minimal when $\xi \rightarrow 0$ so that the Landau gauge turns out to be the optimal choice for any fixed strong coupling α_s , as already found in scalar QED[42].

The plot of the GEP was shown in Fig. 3. In Landau gauge Eq.(31) gives

$$\frac{V_G(m)}{2N_A} = \frac{m^4}{128\pi^2} \left[\alpha \left(\log \frac{m^2}{m_0^2} \right)^2 + 2 \log \frac{m^2}{m_0^2} - 1 \right] \quad (63)$$

which is the renormalized GEP in units of the optimal gluon-mass parameter m_0 and is shown in Fig. 4. The figure shows the existence of two competing stationary points for the vacuum: an unstable local minimum at $m = 0$ and a deeper stable minimum at $m = m_0$.

The existence of a stable massive vacuum is a remarkable non-perturbative prediction of the present variational method and can be regarded as a proof of mass generation in pure Yang-Mills theory. We are tempted to identify the unstable stationary point at $m = 0$ with the massless scaling solution of Schwinger-Dyson equations. That solution is not found in lattice simulations. We observe that if we take $d = 2$ in Eqs.(58),(60), the effective potential becomes positive with a stable minimum at $m = 0$, so that no generation of mass is predicted for the two-dimensional theory.

In the next section, we will show that the two minima acquire a very different behavior at finite temperature. The massless vacuum at $m = 0$ develops a thermal mass that increases with temperature like for a standard massless boson, while the minimum at $m = m_0$ shows a decrease of the mass until a weak first order transition occurs before the merging of the minima.

In the present calculation we ignore the running of the coupling even if it is known that α_s changes in the range $0.4 < \alpha_s < 1.2$ below 2 GeV[38]. However, as shown in Fig. 4, when written in physical units of m_0 , the renormalized GEP is not very sensitive to the actual value of the strong coupling α_s , especially at the local minima that are identified as the physical configurations. Thus everything seems to be fixed by the physical scale m_0 .

Since there is no scale in the original Lagrangian, the actual value of the mass m_0 cannot be predicted by the theory and must come from the phenomenology. The massive expansion of Refs.[38, 39] arises as the natural expansion around the best trial massive vacuum at $m = m_0$. By that expansion, at one loop, the gluon propagator was found in perfect agreement with the data of lattice simulations[41]. The inverse dressing function, which is basically given by the gluon self-energy, is determined without any free parameter and is not monotone, with a pronounced minimum that allows us to fix the energy scale with good accuracy. Sharing the same units of the lattice data, the scale $m_0 = 0.73$ GeV is extracted for $N = 3$ [38, 41]. We will use that scale in the next sections.

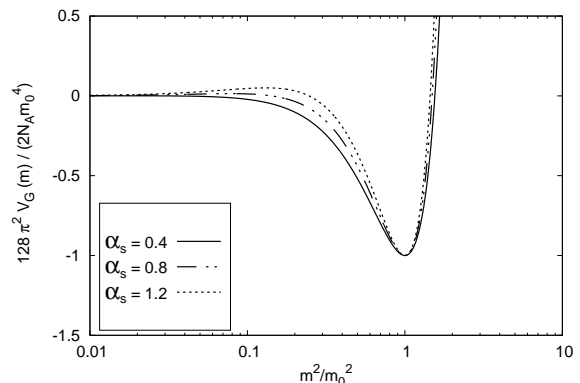


Figure 4: The renormalized GEP of Eq.(63) is shown in units of m_0 for different values of the strong coupling α_s .

IV. THE GEP AT FINITE TEMPERATURE AND DECONFINEMENT

At finite temperature, because of Jensen-Feynman inequality, Eq.(11), the first-order free energy is bounded below by the exact free energy $\mathcal{F}(T)$ that can be expressed as

$$e^{-\beta[\mathcal{V}_3 \mathcal{F}(T)]} = \int \mathcal{D}_{A,\omega} e^{(S_0 + S_{int})} \quad (64)$$

where the thermal action is the integral over imaginary time defined in Eq.(9). If we split the action as in the previous section, inserting the mass terms Eqs.(46),(49) in the free part and the counterterms Eqs.(53) among the vertices, the free energy in Eq.(64) is expanded by the same formal massive expansion as before. The first-order approximation $\mathcal{F}_1(T, m)$ depends on the mass parameter m and is given by the same graphs in the second row of Fig. 1. When optimized it gives the GEP, while the optimal value of m that minimizes $\mathcal{F}_1(T, m)$ provides the best trial mass parameter $m(T)$ at finite temperature, so that $m(0) = m_0$.

The sum of one-loop graphs is still given by Eq.(58) where the integrals K , J in Eq.(18) now include a sum over discrete frequencies and their explicit expressions in Eq.(20) are replaced by

$$K(T, m) = \frac{1}{2}T \sum_n \int \frac{d^3\mathbf{p}}{(2\pi)^3} \log(\mathbf{p}^2 + \omega_n^2 + m^2)$$

$$J(T, m) = T \sum_n \int \frac{d^3\mathbf{p}}{(2\pi)^3} \frac{1}{\mathbf{p}^2 + \omega_n^2 + m^2} \quad (65)$$

having used in Eq.(18) the massive free propagator

$$\Delta_m(\omega_n, \mathbf{p}) = \frac{1}{\mathbf{p}^2 + \omega_n^2 + m^2} \quad (66)$$

in the Euclidean space where $p^\mu = (\omega_n, \mathbf{p})$ and $\omega_n = 2\pi nT$. In the limit $T \rightarrow 0$ the vacuum integrals in Eqs.(20) are recovered as $J(m) = J(0, m)$ and $K(m) = K(0, m)$. We denote them by $J_V(m)$ and $K_V(m)$, respectively. They contain the diverging part of the integrals and can be regularized as discussed in the previous sections. Their explicit expression is given by Eqs.(29). The thermal parts are finite but depend on T . We denote them by $J_T(T, m)$ and $K_T(T, m)$, respectively. Omitting the arguments for brevity, they can be written by an explicit calculation as

$$K_T = K - K_V = -\frac{1}{6\pi^2} \int_0^\infty \frac{n(\epsilon_{k,m})}{\epsilon_{k,m}} k^4 dk$$

$$J_T = J - J_V = \frac{1}{2\pi^2} \int_0^\infty \frac{n(\epsilon_{k,m})}{\epsilon_{k,m}} k^2 dk \quad (67)$$

where $\epsilon_{k,m} = \sqrt{k^2 + m^2}$ and $n(\epsilon) = [\exp(\beta\epsilon) - 1]^{-1}$ is the Bose distribution. Setting $d = 4$ in Eq.(58), the first-order free energy $\mathcal{F}_1(T, m)$ reads

$$\mathcal{F}_1(T, m) = 2N_A \left[K - \frac{1}{2}m^2 J \right] + \mathcal{F}_{2L}(T, m) \quad (68)$$

where $\mathcal{F}_{2L}(T, m)$ is the two-loop graph in the second row of Fig. 1. Because of the breaking of Lorentz invariance at finite T , its expression gets formally different than the vacuum term in Eq.(60).

Following the same steps of the previous sections, in the Landau gauge, the seagull graph of the gluon self energy can be written as[65]

$$\Pi_{ab}^{\mu\nu} = -\delta_{ab} N g^2 T \sum_n \int \frac{d^3\mathbf{p}}{(2\pi)^3} [2\delta^{\mu\nu} \Delta_m + p^\mu p^\nu \Delta_0 \Delta_m] \quad (69)$$

where $\Delta_m = \Delta_m(p)$ is the Euclidean propagator in Eq.(66). Integrating the single terms, it can be written as

$$\Pi_{ab}^{\mu\nu} = -\delta_{ab} N g^2 [2\delta^{\mu\nu} J + I^{\mu\nu}] \quad (70)$$

where

$$I^{\mu\nu} = T \sum_n \int \frac{d^3\mathbf{p}}{(2\pi)^3} p^\mu p^\nu \Delta_m(p) \Delta_0(p). \quad (71)$$

The trace of $I^{\mu\nu}$ is $I^{\mu\mu} = J$, so that at $T = 0$, by Lorentz invariance, the self energy of Eq.(59) is recovered for $d = 4$. At finite temperature, $I^{\mu\nu}$ is still diagonal but $I^{00} \neq I^{ii}$. By rotational invariance, using the trace again, we can write

$$I^{11} = I^{22} = I^{33} = \frac{1}{3} (J - I^{00}) \quad (72)$$

which holds separately for the thermal and vacuum parts. While the vacuum part is just $I_V^{00} = I_V^{ii} = J_V/4$, the thermal part can be obtained by an explicit integration as

$$I_T^{00} = \frac{1}{m^2} (h_m - h_0) \quad (73)$$

where h_m is the integral

$$h_m = \frac{1}{2\pi^2} \int_0^\infty \epsilon_{k,m} n(\epsilon_{k,m}) k^2 dk \quad (74)$$

that can be evaluated exactly for $m = 0$ yielding $h_0 = \pi^2 T^4/30$.

Closing the second loop with the transverse gluon propagator ($\xi = 0$) and inserting the symmetry factor $1/4$

$$\mathcal{F}_{2L} = \frac{1}{4} \Pi_{ab}^{\mu\nu} T \sum_n \int \frac{d^3\mathbf{p}}{(2\pi)^3} \Delta_m(p) t_{\mu\nu}(p) \delta_{ab}. \quad (75)$$

Then, using Eq.(70), the two-loop term reads

$$\mathcal{F}_{2L} = \frac{N_A N g^2}{4} (7J^2 - I^{\mu\nu} I^{\mu\nu}) \quad (76)$$

and its inclusion in Eq.(68) gives the first-order free energy in closed form. When optimized, it provides the GEP at finite temperature. With some abuse of language

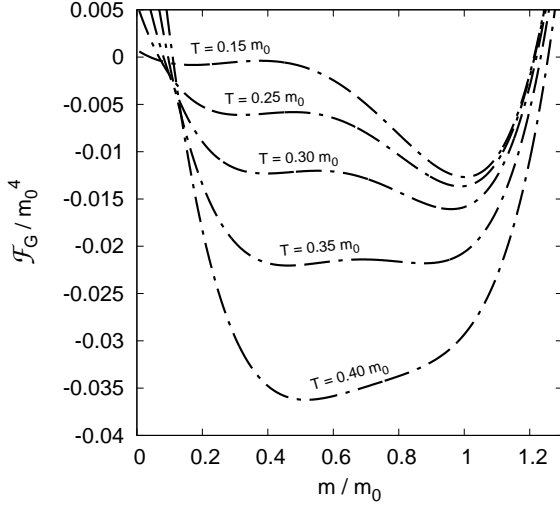


Figure 5: The renormalized GEP of Eqs.(77),(78) is shown in units of m_0 for $\alpha_s = 1$ and different values of the temperature.

we can denote the first-order free energy by $\mathcal{F}_G(T, m)$ and call it the GEP.

It is useful to separate the thermal and vacuum parts of the GEP. If we do that and use the explicit renormalized expressions Eqs.(29) for the vacuum parts J_V, K_V , the total first-order free energy of Eqs.(68), (76) can be easily shown to become

$$\mathcal{F}_G(T, m) = \mathcal{F}_G(0, m) + \delta\mathcal{F}_G(T, m) \quad (77)$$

where the vacuum part $\mathcal{F}_G(0, m) = V_G(m)$ is just the GEP at $T = 0$, given by Eq.(63) when expressed in terms of m_0 . The thermal part $\delta\mathcal{F}_G(T, m)$ vanishes at $T = 0$ and can be written as

$$\begin{aligned} \frac{\delta\mathcal{F}_G(T, m)}{2N_A} = & K_T + \frac{\alpha m^2}{4} J_T \log \frac{m^2}{m_0^2} \\ & + 2\pi^2\alpha \left[J_T^2 - \left(\frac{2}{3}\right)^4 \left(\frac{J_T}{4} - I_T^{00}\right)^2 \right]. \end{aligned} \quad (78)$$

The GEP is shown in Fig. 5 for different values of the temperature and in Fig. 6 for several values of the coupling α_s . As already discussed in the previous sections, the GEP is not very sensitive to the coupling, especially in the physical ranges around the minima. Thus, while α_s is expected to run in the range $0.4 < \alpha_s < 1.2$ below 2 GeV[4, 38], we will keep α_s fixed at the reasonable value $\alpha_s = 1$ in the following discussion. We checked that any other choice does not introduce any important change in the results.

At finite temperature, we observe that the minima of the GEP have a very different behavior. The absolute minimum at $m = m_0$ is almost frozen when $T \ll m_0$, as expected for a massive confined gluon. When the temperature increases the minimum moves backwards, so that the optimal mass parameter $m(T)$ is a decreasing function of the temperature, in fair agreement with

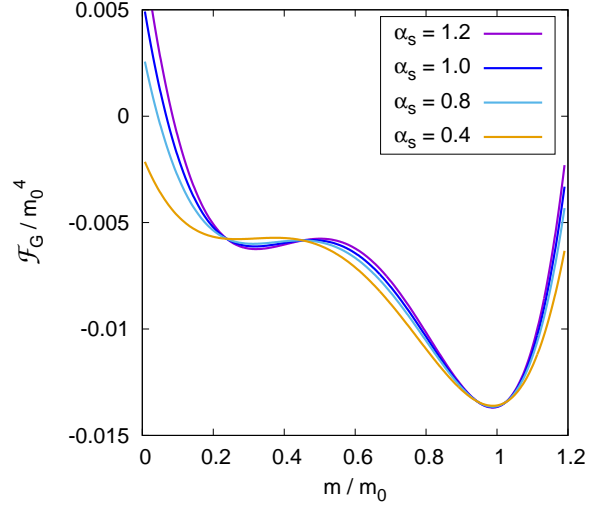


Figure 6: The renormalized GEP of Eqs.(77),(78) is shown in units of m_0 for $T/m_0 = 0.25$ and different values of the strong coupling α_s .

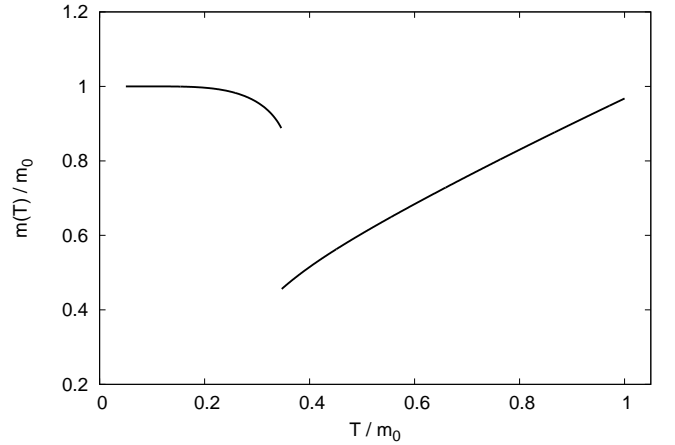


Figure 7: The optimal mass parameter $m(T)$ which minimizes the GEP is shown as a function of temperature for $\alpha_s = 1$.

the decrease of mass that is observed on the lattice below T_c [10]. The unstable minimum, at $m = 0$ in Fig. 4, moves forward when $T > 0$ and its mass value increases almost linearly like the thermal mass of a massless boson. It gets deeper with increasing temperature. Thus the GEP seems to show the competition between a confined boson with a dynamical mass and a free boson with a thermal mass. As shown in Fig. 5, at a critical temperature $T_c \approx 0.35m_0$ the minima reach the same free energy before they can merge, so that a weak first-order phase transition is predicted with a discontinuous drop of the optimal mass parameter $m(T)$ that is displayed in Fig. 7. The free energy at the minima is shown in Fig. 8 across the transition. Below the transition point, the upper curve is the GEP at the unstable thermal mass, while the lower curve is the GEP at the stable dynamical

mass. Above the transition point they reverse. At any temperature, the physical free energy is the lower curve $\mathcal{F}_G(T, m(T))$. The equation of state can be studied by introducing pressure and entropy density according to

$$\begin{aligned} p &= -\mathcal{F}_G(T, m(T)) \\ s &= -\frac{\partial}{\partial T} \mathcal{F}_G(T, m(T)). \end{aligned} \quad (79)$$

and is shown in units of T_c in Fig. 9 together with the recent lattice data of Ref.[67] which are consistent with previous existing data[68, 69]. We observe that because of the full cancellation of the unphysical degrees of freedom, the free energy is decreasing, as it should be, so that the pressure is an increasing function of temperature and the entropy is always positive, at variance with phenomenological one-loop calculations[32, 34]. The small jump of the entropy density at $T = T_c$ is $\Delta s/T_c^3 = 1.73$ yielding a latent heat $\Delta H_0 = 1.73 T_c^4$ which is not too far from the values $1.3 - 1.5$ found in lattice simulations[67–69].

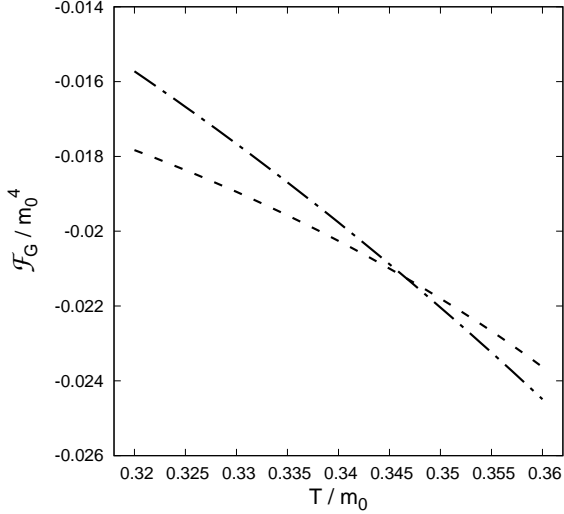


Figure 8: The Free energy at the minima of the GEP across the transition for $\alpha_s = 1$. Below the transition point, the upper curve (dot-dashed) is the GEP at the unstable thermal mass while the lower curve (dashed) is the GEP at the stable dynamical mass. The order reverses above the transition point.

The slight effect of a change of α_s on the critical temperature is less than $\pm 1\%$ and is shown in Fig. 10 at a very enlarged scale. Taking an average value $T_c = 0.347$ and using the scale $m_0 = 0.73$ GeV that arises for $N = 3$ from the massive expansion at one-loop[36–39], we predict $T_c = 253$ MeV, which is very close to the value $T_c = 270$ MeV that is found on the lattice[10].

It is remarkable that at the lowest order of approximation, by a simple variational calculation, the method provides estimates for T_c and latent heat that are very close to the exact values, with an overall description of the equation of state that is in qualitative agreement with the data of simulations, without unphysical features like

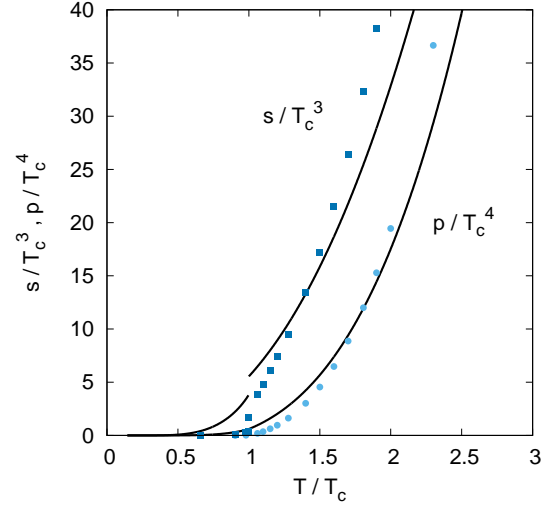


Figure 9: Equation of state. The pressure and entropy densities are evaluated by Eqs.(79) for $\alpha_s = 1$ and are shown in units of T_c (solid lines). The circles and the squares are the lattice data of Ref.[67] for pressure and entropy, respectively.

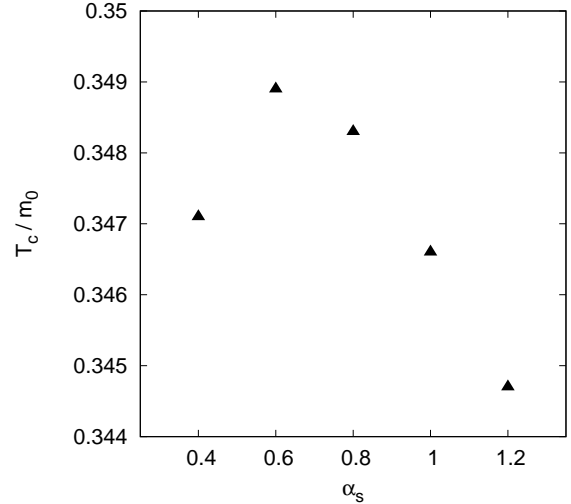


Figure 10: The critical temperature is shown at a very enlarged scale, as a function of the coupling α_s . The minor effect of its change is less than $\pm 1\%$.

negative entropy and without any fit parameter, from first principles. That is more than one would expect from a simple free-particle massive propagator Δ_m . However, we observe that in Fig. 9, strong deviations from the lattice data emerge in the critical region, with an enhancement of the thermodynamic functions below the transition and an underestimate of the same functions above the transition. The details of the equation of state are better shown by a plot of the normalized densities s/T^3 and p/T^4 . In Fig. 11 the normalized entropy density is shown together with the lattice data of Ref.[67]. While the jump at the critical temperature is slightly

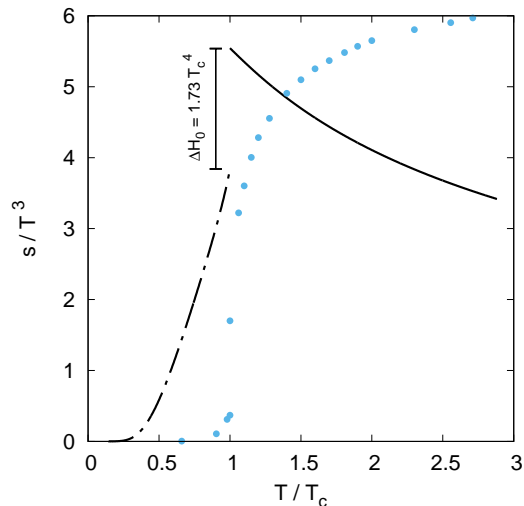


Figure 11: The normalized entropy density s/T^3 is evaluated by Eq.(79) below the transition (broken line) and above it (solid line) for $\alpha_s = 1$. The circles are the lattice data of Ref.[67].

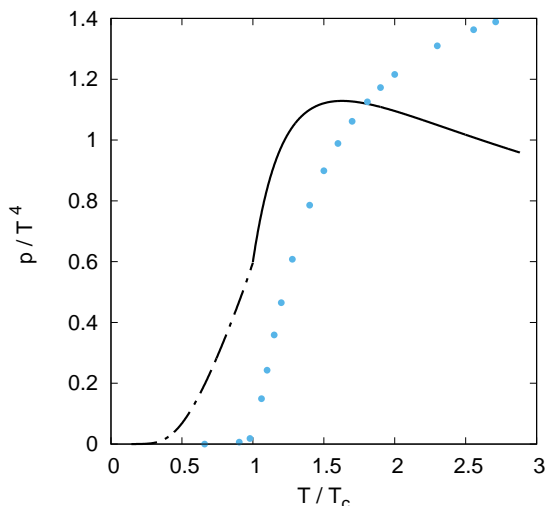


Figure 12: The normalized pressure density p/T^4 is evaluated by Eq.(79) below the transition (broken line) and above it (solid line) for $\alpha_s = 1$. The circles are the lattice data of Ref.[67].

larger than predicted on the lattice, the normalized entropy is too large below the transition and has the wrong decreasing behavior above T_c . The same features can be observed for the normalized pressure density in Fig. 12. By some compensation, the trace anomaly $I = sT - 4p$ in Fig. 13 has the correct qualitative behavior.

Eventually, we expect that the overall picture of dynamical mass generation, deconfinement transition and equation of state would improve greatly by adding higher-order terms of the expansion in the free energy, as it is

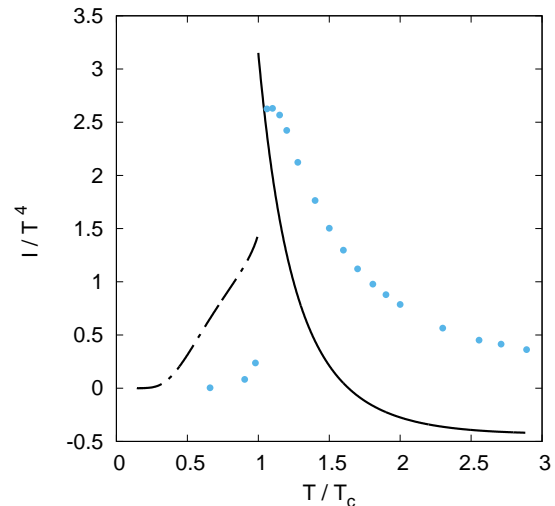


Figure 13: The normalized trace anomaly $I/T^4 = (sT - 4p)/T^4$ is evaluated by Eq.(79) below the transition (broken line) and above it (solid line) for $\alpha_s = 1$. The circles are the lattice data of Ref.[67].

the case for the dressed propagator which gets on top of the lattice data when the one-loop terms are added to the zeroth-order massive propagator Δ_m [38, 39, 41].

V. DISCUSSION

The self-consistency gap equation of the GEP, Eq.(25) has attracted a lot of attention in the past[19, 20, 44] as a basic physical tool for explaining the dynamical mass generation of Yang-Mills theories. The main difficulty of handling the gap equation has always been the regularization of the diverging integral $J(m)$ and its physical meaning. Here we adopt a very simple scheme based on dimensional regularization, yielding a bounded GEP with two minima. The existence of a deeper minimum at $m = m_0 \neq 0$ can be regarded as a variational proof of mass generation in the original scale-less theory.

In order to enforce our confidence on the genuine physical nature of the minimum, we explored the model at finite temperature. The emerging scenario for the equation of state and the deconfinement transition is in very good qualitative agreement with the data of lattice simulations, leaving no doubt about the physical interpretation of the minima in the GEP.

Moreover, the method provides a perturbative tool for improving the results order by order. The expansion around the optimal vacuum of the GEP turns out to be the massive expansion developed in Refs.[37–39] which provides accurate and analytical expressions for the propagators at one-loop already. Once the non-perturbative effects are embedded in the optimal variational mass, the residual interaction can be described by perturbation theory yielding a powerful analytical tool for QCD in the IR.

Thus, we argue that the present variational estimate of the thermodynamical potentials might be improved by inclusion of higher order terms. Second order extensions of the GEP have been discussed by several authors[55–58]. In general, they do not retain the genuine variational property of the GEP but different optimization strategies have been proposed ranging from the principle of minimal sensitivity[60] to the method of minimal variance[62–65]. Explicit massive two-loop thermal graphs have been evaluated in Ref.[34]. Here, we limited the calculation at the first order, just because we preferred to maintain the genuine variational nature of the method unspoiled, according to Jensen-Feynman inequality. Nevertheless, the pure GEP provides a remarkably good picture of the deconfinement transition. From first principles, without any fit parameter, the simple first-order calculation predicts a weak first order transition at $T_c \approx 250$ MeV for $N = 3$, with a small latent heat $\Delta H_0 \approx 1.7 T_c$ which is only slightly larger than predicted on the lattice. The details of the equation of state are not reproduced with the same accuracy, which is not surprising at first order. Moreover, the method fails to predict a continuous transition for $N = 2$. That could be the consequence of a known issue for the GEP which is known to predict a weak first-order transition even when the transition is second-order for the scalar theory[45, 55]. In that case, a continuous transition is restored by inclusion of second order terms[55]. Moreover, the GEP is known[42] to predict the correct $N \rightarrow \infty$ limit of $1/N$ expansions, so that its reliability increases when N is large.

An important limitation of the present study arises from the use of a fixed coupling α_s . While the results are almost insensitive to the running in the IR, important deviations are expected above 2 GeV, so that we had to limit the discussion at the transition range. How-

ever, for large energies and $T \gg m_0$ the effects of the finite mass become negligible and the standard results of perturbation theory must be recovered. Eventually, the correct matching between IR and UV can be included in the formalism by use of the renormalization group equations. On the other hand, when limiting the study in the low temperature range $T < m_0$, no resummation of hard thermal loops is required because of the finite mass in the loops.

At variance with some phenomenological one-loop calculations where a mass parameter is inserted by hand in the Lagrangian[32, 34], here the entropy is never negative, as it should be. That is because we ensured that the unphysical degrees of freedom are canceled by the ghost. That can only happen if all the trial propagators are massive with the same mass. We have the freedom to take a massive trial ghost propagator because the mass parameter is subtracted in the interaction, leaving the total Lagrangian unchanged, while a phenomenological mass for the ghost would be at odds with the lattice data for the dressed ghost propagator. One could wonder if the inclusion of a mass parameter in the trial ghost propagator could shift the pole of the ghost at one-loop and make it massive. However, in the massive expansion of the propagators[38, 39] the counterterm cancels the shift at tree level and any real mass term can only arise from loops. That is the reason why no mass would arise for the photon in QED by the same method. It can be easily shown[65] that the ghost self energy is of order $\mathcal{O}(p^2)$ and vanishes when the external momentum $p \rightarrow 0$, so that the dressed ghost propagator still has a pole at $p^2 = 0$. That is an other way to see that the gluon mass arises from gluon loops in the expansion and is not a mere shift by a mass parameter.

-
- [1] A. G. Duarte, O. Oliveira, P. J. Silva, Phys. Rev. D **94**, 014502 (2016).
 - [2] A. Cucchieri and T. Mendes, Phys. Rev. D **78**, 094503 (2008).
 - [3] A. Cucchieri and T. Mendes, Phys. Rev. Lett. **100**, 241601 (2008).
 - [4] I.L. Bogolubsky, E.M. Ilgenfritz, M. Muller-Preussker, A. Sternbeck, Phys. Lett. B **676**, 69 (2009).
 - [5] D. Dudal, O. Oliveira, N. Vandersickel, Phys. Rev. D **81**, 074505 (2010).
 - [6] A. Ayala, A. Bashir, D. Binosi, M. Cristoforetti and J. Rodriguez-Quintero, Phys. Rev. D **86**, 074512 (2012).
 - [7] O. Oliveira, P. J. Silva, Phys. Rev. D **86**, 114513 (2012).
 - [8] G. Burgio, M. Quandt, H. Reinhardt, H. Vogt, Phys. Rev. D **92**, 034518 (2015).
 - [9] B. Lucini, M. Teper, U. Wenger, JHEP **01**, 061 (2004).
 - [10] P. J. Silva, O. Oliveira, P. Bicudo, N. Cardoso, Phys. Rev. D **89**, 074503 (2014).
 - [11] R. Aouane, V. Bornyakov, E.-M. Ilgenfritz, V. Mitrushkin, M. Müller-Preussker, A. Sternbeck, Phys. Rev. D **85**, 034501 (2012).
 - [12] F. Marhauser and J. M. Pawłowski, arXiv:0812.1144.
 - [13] J. Braun, H. Gies and J. M. Pawłowski, Phys. Lett. B **684**, 262 (2010).
 - [14] J. Braun, A. Eichhorn, H. Gies and J. M. Pawłowski, Eur. Phys. J. C **70**, 689 (2010).
 - [15] L. Fister and J. M. Pawłowski, Phys. Rev. D **88**, 045010 (2013).
 - [16] D. Epple, H. Reinhardt and W. Schleifenbaum, Phys. Rev. D **75**, 045011 (2007).
 - [17] R. Alkofer, C. S. Fischer and F. J. Llanes-Estrada, Mod. Phys. Lett. A **23**, 1105 (2008).
 - [18] C. S. Fischer, Phys. Rev. Lett. **103**, 052003 (2009).
 - [19] A. C. Aguilar, D. Binosi, and J. Papavassiliou, Phys. Rev. D **78**, 025010 (2008).
 - [20] A. C. Aguilar and J. Papavassiliou, Phys. Rev. D **81**, 034003 (2010).
 - [21] A. C. Aguilar, D. Binosi, and J. Papavassiliou, Phys. Rev. D **89**, 085032 (2014).
 - [22] A. C. Aguilar, D. Binosi, D. Ibanez, and J. Papavassiliou, Phys. Rev. D **90**, 065027 (2014).
 - [23] A. C. Aguilar, D. Binosi, and J. Papavassiliou, Phys. Rev.

- D **91**, 085014 (2015).
- [24] H. Reinhardt and J. Hefner, Phys. Lett. B **718**, 672 (2012); Phys. Rev. D **88**, 045024 (2013).
 - [25] D. Zwanziger, Nucl. Phys. B **323**, 513 (1989).
 - [26] D. Dudal, J. A. Gracey, S. P. Sorella, N. Vandersickel, H. Verschelde, Phys. Rev. D **78**, 065047 (2008).
 - [27] D. Dudal, S. P. Sorella, N. Vandersickel, H. Verschelde, Phys. Rev. D **77**, 071501 (2008).
 - [28] D. Dudal, S. P. Sorella, N. Vandersickel, Phys. Rev. D **84**, 065039 (2011).
 - [29] M. Tissier, N. Wschebor, Phys. Rev. D **82**, 101701(R) (2010).
 - [30] M. Tissier, N. Wschebor, Phys. Rev. D **84**, 045018 (2011).
 - [31] U. Reinosa, J. Serreau, M. Tissier and N. Wschebor, Phys. Rev. D **89**, 105016 (2014).
 - [32] U. Reinosa, J. Serreau, M. Tissier and N. Wschebor, Phys. Lett. B **742**, 61 (2015).
 - [33] U. Reinosa, J. Serreau, M. Tissier and N. Wschebor, Phys. Rev. D **91**, 045035 (2015).
 - [34] U. Reinosa, J. Serreau and M. Tissier, Phys. Rev. D **92**, 025021 (2015).
 - [35] U. Reinosa, J. Serreau, M. Tissier, N. Wschebor, Phys. Rev. D **93**, 105002 (2016).
 - [36] F. Siringo, in *Correlations in Condensed Matter under Extreme Conditions*, edited by G.G.N. Angilella and A. La Magna (Springer International Publishing AG, 2017); F. Siringo, arXiv:1701.00286.
 - [37] F. Siringo, *Perturbative study of Yang-Mills theory in the infrared*, arXiv:1509.05891.
 - [38] F. Siringo, Nucl. Phys. B **907**, 572 (2016), [arXiv:1511.01015].
 - [39] F. Siringo, Phys. Rev. D **94**, 114036 (2016), [arXiv:1605.07357].
 - [40] F. Siringo, *Quasigluon lifetime and confinement from first principles*, arXiv:1705.06160.
 - [41] F. Siringo, EPJ Web of Conferences **137**, 13016 (2017), [arXiv:1607.02040].
 - [42] R. Ibáñez-Meier, I. Stancu, P.M. Stevenson, Z. Phys. C **70**, 307 (1996).
 - [43] J. M. Cornwall, R. Jackiw and E. Tomboulis, Phys. Rev. D **10**, 2428 (1974).
 - [44] J.M. Cornwall, Phys. Rev. D **26**, 1453 (1982).
 - [45] P.M. Stevenson, Phys. Rev. D **32**, 1389 (1985).
 - [46] P. M. Stevenson, G. A. Hajj, J. F. Reed, Phys. Rev. D **34**, 3117 (1986).
 - [47] F. Siringo, Phys. Rev. D **62**, 116009 (2000).
 - [48] F. Siringo, Europhys. Lett. **59**, 820 (2002).
 - [49] F. Siringo and L. Marotta, Int. J. Mod. Phys. **A25**, 5865 (2010), [arXiv:0901.2418v2].
 - [50] F. Siringo, L. Marotta, Phys. Rev. D **78**, 016003 (2008).
 - [51] F. Siringo and L. Marotta, Phys. Rev. D **74**, 115001 (2006).
 - [52] M. Camarda, G.G.N. Angilella, R. Pucci, F. Siringo, Eur. Phys. J. B **33**, 273 (2003).
 - [53] L. Marotta, M. Camarda, G.G.N. Angilella and F. Siringo, Phys. Rev. B **73**, 104517 (2006).
 - [54] L. Marotta and F. Siringo, Mod. Phys. Lett. B, **26**, 1250130 (2012), [arXiv:0806.4569v3].
 - [55] I. Stancu and P. M. Stevenson, Phys. Rev. D **42**, 2710 (1990).
 - [56] F. Siringo, Phys. Rev. D **88**, 056020 (2013), arXiv:1308.1836.
 - [57] F. Siringo, Phys. Rev. D **86**, 076016 (2012), [arXiv:1208.3592v2].
 - [58] I. Stancu, Phys. Rev. D **43**, 1283 (1991).
 - [59] P. Cea, L. Tedesco, Phys. Rev. D **55**, 4967 (1997).
 - [60] P.M. Stevenson, Phys. Rev. D **23**, 2916 (1981).
 - [61] F. Siringo and L. Marotta, Eur. Phys. J. C **44**, 293 (2005).
 - [62] F. Siringo, Mod. Phys. Lett. A **29**, 1450026 (2014), arXiv:1308.4037.
 - [63] F. Siringo, Phys. Rev. D **89**, 025005 (2014), arXiv:1308.2913.
 - [64] F. Siringo, Phys. Rev. D **90**, 094021 (2014), arXiv:1408.5313.
 - [65] F. Siringo, Phys. Rev. D **92**, 074034 (2015), arXiv:1507.00122.
 - [66] S. Coleman, E. Weinberg, Phys. Rev. D **7**, 1888 (1973).
 - [67] L. Giusti and M. Pepe, Phys. Lett. B **769**, 385 (2017).
 - [68] Sz. Borsányi, G. Endrodi, Z. Fodor, S. D. Katz, K. K. Szabó, JHEP **1207**, 056 (2012).
 - [69] G. Boyd, J. Engels, F. Karsch, E. Laermann, C. Legeland, M. Luetgemeier, B. Petersson, Nucl. Phys. B **469**, 419 (1996).